IEEE Photonics Journal
An IEEE Photonics Society Publication

Grating-Assisted Directional Coupler in Lithium Niobate for Tunable Mode Filtering

Volume 13, Number 2, April 2021

Jun Hui Li
Mao Hui Zhou
Hao Yao
Meng Ke Wang
Jie Yun Wu
Kai Xin Chen

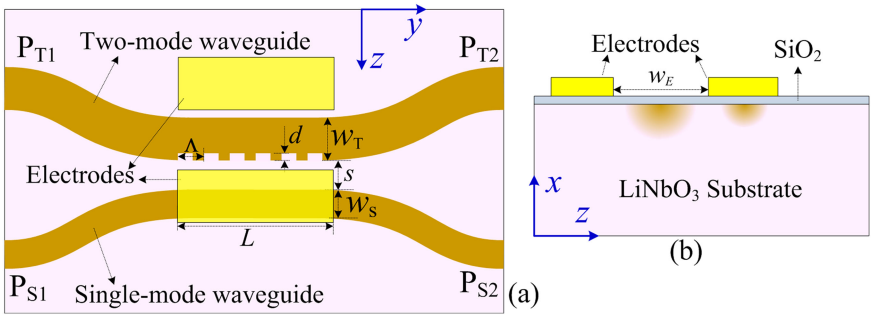

DOI: 10.1109/JPHOT.2021.3061089

Grating-Assisted Directional Coupler in Lithium Niobate for Tunable Mode Filtering

Jun Hui Li, Mao Hui Zhou, Hao Yao, Meng Ke Wang, Jie Yun Wu, and Kai Xin Chen

School of Optoelectronic Science and Engineering, University of Electronic Science and Technology of China, Chengdu 611731, China

DOI:10.1109/JPHOT.2021.3061089

Manuscript received January 4, 2021; revised February 15, 2021; accepted February 18, 2021. Date of publication February 23, 2021; date of current version March 12, 2021. This work was supported in part by the National Natural Science Foundation of China under Grants 62075027 and U20A20165, in part by the Key R & D Program of Sichuan Province under Grant 2020YFSY0003, in part by the Opened Fund of the State Key Laboratory of Integrated Optoelectronics, under Grant IOSKL2018KF12, and in part by the Fundamental Research Funds for the Central Universities under Grants ZYGX2019J050 and ZYGX2020ZB015. Corresponding author: Kai Xin Chen (e-mail: chenkx@uestc.edu.cn).

Abstract: We propose a long-period grating assisted directional coupler in lithium niobate (LN) for the realization of electro-optic tunable mode filtering functionality. Our typical device, fabricated with the annealed proton-exchange process and designed for filtering out the fundamental mode in a two-mode LN waveguide, achieves a maximum mode extinction ratio of 29 dB at 1551.7 nm wavelength and a –20 dB bandwidth of ∼2.5 nm with an electrical wavelength tuning sensitivity of 0.182 nm/V.

Index Terms: Grating-assisted directional coupler, lithium niobate, electro-optic tuning, mode filter, mode-division multiplexing.

1. Introduction

A mode filter capable of eliminating undesirable modes and extracting the desired ones, resembling wavelength filter for wavelength-division multiplexing (WDM), is an essential component for the realization of mode discrimination functionality in mode-division multiplexing (MDM) optical communication systems [1]–[7]. In view of the fact that higher-order modes in a waveguide can be easily filtered out by using a tapered or bent waveguide [1] due to their weak optical confinement, while filtering lower-order modes is difficult because they are well confined in a waveguide. Thus studies are mainly carried out around how to filter out low-order modes, especially the fundamental mode. Nowadays, several types of mode filters using long-period gratings (LPG) [1], graphene embedded waveguides [2], Mach–Zehnder interferometers combined with taper [3] or slot taper [4], Y-junction combined with multimode interference (MMI) [5], photonic crystals [6], and subwavelength grating-based contra-directional coupler [7] have been demonstrated on optical polymer [1]–[3] or silicon-on-insulator (SOI) [4]–[7] platforms.

A grating-assisted directional coupler (GADC) consists of two parallel dissimilar waveguides and a Bragg grating [8]–[12] or a long-period grating [13] formed along one of the two waveguides. Such a coupler enables the coupling between the two same order modes of the two dissimilar waveguides since the introduction of the grating is able to compensate for the phase mismatch of

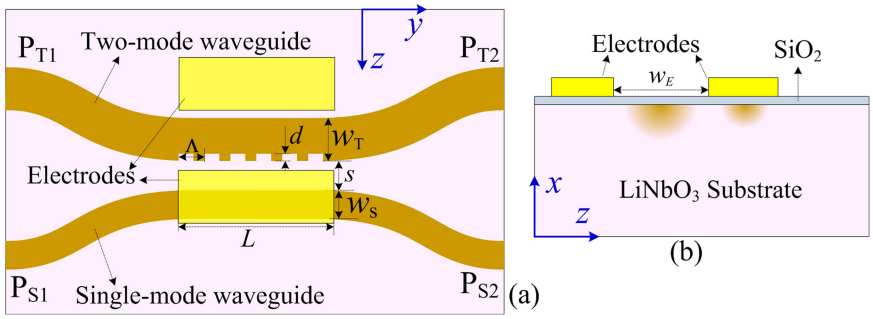

Fig. 1. Schematic diagram (a) and cross-sectional view of the coupling region (b) of the proposed LPGADC.

the two coupled modes. Up to now, GADCs have been proposed as contra-directional coupler [8], add-drop filter [9], polarization splitter [10], resonator [11], or a mode (de)multiplexer [12], [13]. In this paper, we propose and demonstrate an electro-optic (EO) tunable mode filtering functionality implemented with a long-period GADC (LPGADC) in lithium niobate (LN) for the first time, to the best of our knowledge. Previously, we have demonstrated an asymmetric directional coupler [14] and cascaded three dimensional directional couplers [15] in LN, the former is capable of achieving the coupling between the LP_{01} mode in a single-mode waveguide (SMW) and the LP_{11a} mode in a two-mode waveguide (TMW), while the latter realizes not only the coupling between the LP_{01} of the SMW and LP_{11a} modes of the TMW but also the coupling between the LP_{01} of another SMW and LP_{11b} modes of the TMW. Both devices can be used as electro-optic mode-selective switch. Although the adiabatic coupling configuration used in [14] and [15] is capable of realizing mode conversion between the higher-order modes in a multimode waveguide and the fundamental mode in a single mode waveguide, it is difficult to filter out the fundamental mode in a multimode waveguide by coupling it into another waveguide solely with such coupling configurations.

In this work, we further incorporate an LPG into our previously demonstrated asymmetric directional coupler configuration to compensate for the phase mismatch of the two LP_{01} modes in the SMW and the TMW so as to achieve the coupling between them and, hence, implement an EO tunable LP_{01} mode filter. The LPG used here is formed along the inner side of the TMW. The proposed LPGADC can be fabricated with a single photolithography and annealed proton-exchange process, which ease the fabrication process of the device. Our typical fabricated device achieves a maximum mode extinction ratio of 29 dB at 1551.7 nm wavelength and a –20 dB bandwidth of $\sim$2.5 nm with an electrical wavelength tuning sensitivity of 0.182 nm/V. Compared with the above conventional mode filters with fixed operation wavelength, our proposed mode filter offers the strength of flexible design, simple and compact structure, and high-speed tunable wavelength-selective mode filtering functionality, which is advantageous to ease the stringent requirements in the design and fabrication of the filter and increase the flexibility of MDM networks.

2. Device Configuration and Design

Our proposed LPGADC is shown schematically in Fig. 1(a), which is composed of an asymmetric directional coupler, an LPG, and a set of aluminum (Al) electrodes. The directional coupler is formed with an SMW of width w_s, which supports only the LP_{01} mode, and a TMW of width w_T, which supports only the LP_{01} and the LP_{11a} mode. In the coupling region, the two waveguides are parallel and separated by a distance *s.* The LPG, which has a period Λ, a corrugation depth *d,* and a length *L* (equal to the length of electrodes), is formed along the inner side of the TMW. The device is formed on an *x*-cut LN substrate by the conventional annealed proton-exchange (APE) process, in which the two waveguides are placed along y direction. As the APE process increases only the

extraordinary refractive index of the LN crystal, the waveguides here support only the transverse-electric (TE) polarization whose electric field is along *z* direction. The Al electrodes are placed on the two sides of the TMW and a layer of silica is used to prevent light absorption loss induced by the Al electrodes, as shown in Fig. 1(b). Such a device configuration can exploit the largest EO coefficient (r_{33}) of the LN crystal. The device is designed to filter out the LP_{01} mode of the TMW by coupling it into the LP_{01} mode of the SMW. To this end, an LPG is introduced to compensate for the phase mismatch of the two LP_{01} modes in the TMW and the SMW, as mentioned above, and its period is determined by the phase-matching condition

$$\Lambda = \frac{\lambda_0}{N_{T01} - N_{S01}} \tag{1}$$

where N_{T01} and N_{S01} are the effective indices of the two LP_{01} modes of the TMW and the SMW, respectively, and λ_0 is the resonance wavelength at which the mode-coupling effect is the strongest. It should be pointed out that to achieve higher accuracy in calculating N_{T01} the width of the TMW should be considered as (w_T – d/2) due to the impact from the grating [16].

To design the proposed device, firstly, we need to get the effective indices N_{T01} and N_{S01} in coupling region. Here, we follow the method used in our previous work [14] to investigate how the effective indices of the modes in the LN waveguides depend on the waveguide width. For this purpose, we fabricated many sets of trial LN waveguides with different widths using different fabrication parameters. The fabrication process is outlined below. A chromium (Cr) film was first deposited on the surface of an x-cut LN substrate by radio-frequency (RF) sputtering. A photoresist pattern of the desired waveguides along y direction was then formed by standard photolithography and transferred to the Cr film by chemical etching. After the photoresist removed, the patterned LN substrate was submerged in stearic acid (the proton source) for proton exchange. At last, the Cr film was removed and the sample was annealed. The effective indices of the modes in the resultant waveguides were measured with a prism-coupler system (Metricon, Model 2010, equipped with a laser operating at 1538.3 nm) at the wavelength 1538.3 nm [17]. From the measurement results with these trial waveguides, we found that the effective index of the LP_{01} mode of a 6.0-μm-wide SMW was $N_{S01} = 2.1409$ and those of the LP_{01} and the LP_{11a} mode of a 11.0-μm-wide TMW were $N_{T01} = 2.1428$ and $N_{T11a} = 2.1393$, respectively, which could be fabricated with a proton-exchange time of 22 min at 250 °C and an annealing time of 3.6 h at 350 °C. As there is no phase matching between the LP_{01} mode of the SMW and the LP_{11a} mode of the TMW, no significant power transfer between the two modes is expected, which is advantageous for the implementation of a low insertion loss of the LP_{11a} mode. According to the above measured results, the desired widths of the SMW and the TMW used in our device are set to be $w_s = 6.0$ μm and $w_T = (11.0 +$ d/2) μm. With the values of the N_{S01} and N_{T01}, the period of the LPG was calculated to be 816 μm at the resonance wavelength of 1550 nm, a conventional communication wavelength.

To further determine the gap spacing *s*, the depth *d*, and the length *L* of the LPGADC required, we conducted extensive simulations on the performance of the device with the beam-propagation method (OptiBPM) using different values of *s*, *d*, and *L*. The duty cycle of the LPG was set to be 50%. The refractive-index profiles of the two waveguides were carefully tailored to ensure that the effective indices of the waveguides in the simulation were equal to the measured values. From the simulation results, we chose $s = 4.0$ μm, $d = 1.2$ μm (corresponding to $w_T = 11.6$ μm), and $L = 16320$ μm (corresponding to 20 grating periods). With these parameters, the LP_{01} mode of the TMW should be completely coupled to the LP_{01} mode of the SMW at the wavelength 1550 nm. Fig. 2(a) and 2(b) show the propagation dynamics along the coupling section of the proposed LPGADC when the TE-polarized LP_{01} and LP_{11a} modes at 1550 nm are launched respectively into the TMW.

3. Device Fabrication and Characterization

We fabricated the proposed optical waveguide LPGADC with the same APE process as described for the fabrication of the trial waveguides. We followed the design parameters as closely as possible in the fabrication process. Before the Al electrodes were formed on the fabricated LPGADC, we first

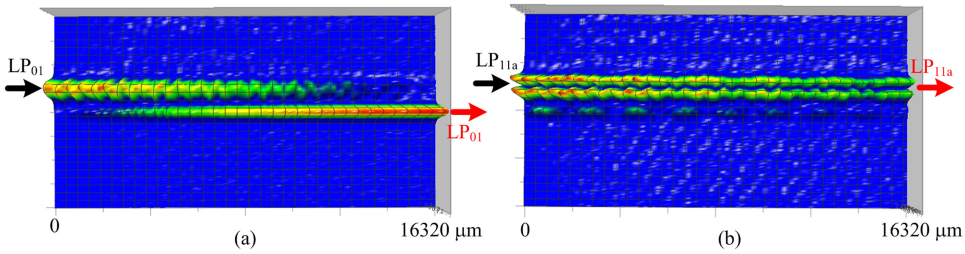

Fig. 2. Propagation dynamics along the coupling region of the proposed LPGADC when the TE-polarized LP_{01} (a) and LP_{11a} (b) modes at 1550 nm are launched into the TMW of the device.

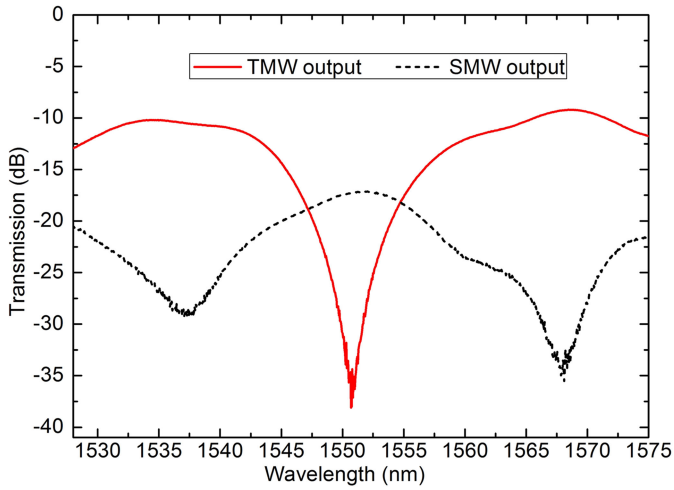

Fig. 3. Transmission spectra from TMW output (P_{T2}) and SMW output (P_{S2}) of a typical fabricated LPGADC measured at 20 °C with broadband light launched into TMW.

investigated the transmission of our fabricated LN LPGADC. After the two ends of the sample were polished carefully, we launched the output light from an amplified spontaneous emission (ASE) source (B&A Technology AS4600) into the input port P_{T1} of the TMW (see Fig. 1) of the device with a lensed single-mode fiber (SMF) through a polarization controller. To excite only the LP_{01} mode of the waveguide, we adjusted the lensed SMF carefully so as to launch the light exactly at the center of the input waveguide. The light from the output port P_{T2} of the TMW or P_{S2} of the SMW was collected by another SMF and monitored by an optical spectrum analyzer (OSA) (Anristu MS97740A). The measured transmission spectra are normalized respectively with respect to the spectrum of fiber to fiber. In view of the fact that the resonance wavelength of the LPGADC is sensitive to the period of the LPG, we fabricated a group of LPGADCs with the same parameters but somewhat different periods on the same LN sample. One of these LPGDACs, which has a period of 818 μm, exhibits the highest performance, and its normalized transmission spectra, measured at 20 °C, are shown in Fig. 3. It can be seen that the transmission spectrum of the TMW exhibits a distinct rejection band with a maximum contrast of 29 dB at the center wavelength 1550.1 nm, while the output spectrum of the SMW exhibits almost complementary pass-band, which indicates that the LP_{01} mode in the TMW is filtered out due to its coupling into the LP_{01} mode of the SMW around the rejection band. To verify this point of view, we next launched the LP_{01} mode at specific wavelengths from a tunable laser (OPEAK DFB-C-WTx) into port P_{T1} of the TMW and took the near-field images of the output light from the port P_{S2} of the SMW and the port P_{T2} of the TMW with an infrared camera (Micron Viewer 7290A). The longest wavelength available with the tunable laser was 1561 nm. The captured images over the wavelength range 1535-1560 nm are shown in Fig. 4(a). At the off-resonance wavelength 1530 nm, the LP_{01} mode launched into the TMW stays in TMW with no

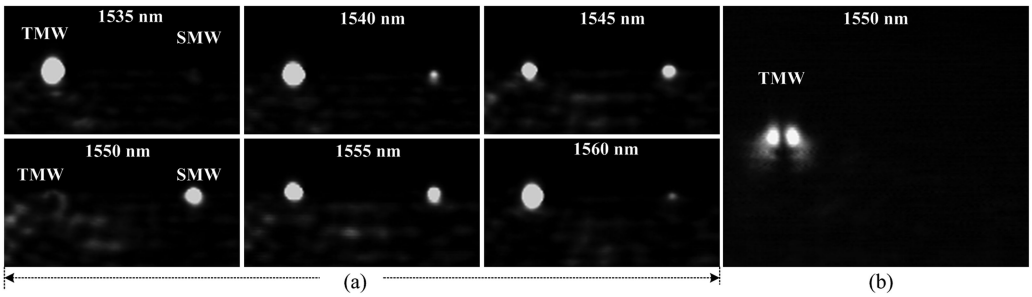

Fig. 4. Output near-field images taken at the output ports P_{T2} of the TMW and P_{S2} of the SMW when the LP_{01} mode at different wavelengths (a) and the LP_{11a} mode at 1550 nm (b) were excited at input port P_{T1} of the TMW.

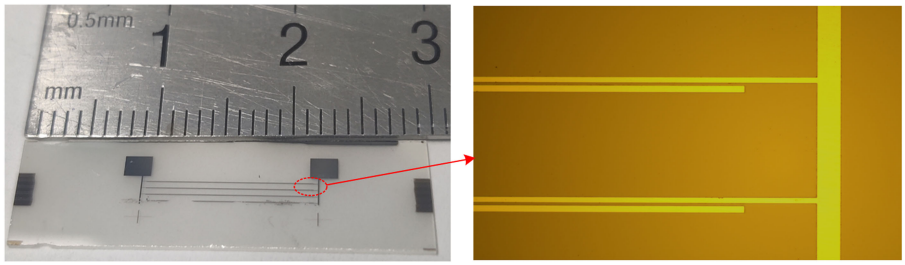

Fig. 5. A photograph of our typical fabricated sample and a microscope image of the electrodes.

measureable light coupled into the LP_{01} mode of the SMW. As the wavelength moves towards the longer wavelength, the LP_{01} mode in the TMW is gradually coupled into the LP_{01} mode of the SMW, and a complete coupling is achieved at 1550 nm, which confirms that the rejection band shown in Fig. 3 is caused by the coupling of the LP_{01} modes of the TMW into the LP_{01} mode of the SMW.

We next verified that the LP_{11a} mode of the TMW would stay in and output from the TMW as the LP_{11a} mode at 1550 nm, the wavelength that the LP_{01} mode would be filtered out. To excite the LP_{11a} mode at input port P_{T1} of the TMW, we adjusted the lensed SMF carefully to introduce a suitable offset from the center of the core and a small tilt angle from the core axis. The output near-field patterns from the TMW and the SMW were also taken by the camera and shown in Fig. 4(b). A clear pattern of LP_{11a} mode was captured and no any other mode pattern was output from the SMW, as shown in Fig 4(b). All of these results confirm that our fabricated LN LPGADC is capable of eliminating the LP_{01} mode at 1550.12 nm while extracting the LP_{11a} mode at the same wavelength.

We then fabricated the Al electrodes on the highest-performance LPGADC to investigate its EO tuning characterization. For this purpose, a layer of $\sim$120 nm thick silica film was first deposited on the surface of the sample by RF magnetron sputtering. Subsequently a layer of $\sim$150 nm thick Al film was evaporated on top of silica and the Al electrodes with a separation of $w_E = 15$ μm was patterned by photolithography and chemical etching process. Fig. 5 shows a photograph of the sample (with a length of 29.5 mm) and a microscope image of the electrodes.

The transmission spectra of the TMW of the highest-performance LPGADC, measured at different tuning voltages, are shown in Fig. 6(a) and (b), where a positive (negative) voltage means that the voltage between the left electrode and the right electrode is positive (negative). The rejection band shifts slightly toward longer wavelengths by $\sim$1.6 nm after the fabrication of the Al electrodes, even though no any tuning voltage is applied to the electrodes. This can be attributed to the slight change of the effective indices of the two LN waveguides due to the deposition of silica. From Fig. 6(a), as the voltage changes from 0 V to -30 V, the rejection band shifts from 1551.8 nm to 1545.8 nm with the contrast dropping from 29 dB at 0 V to 22 dB at -30 V. On the other hand, from

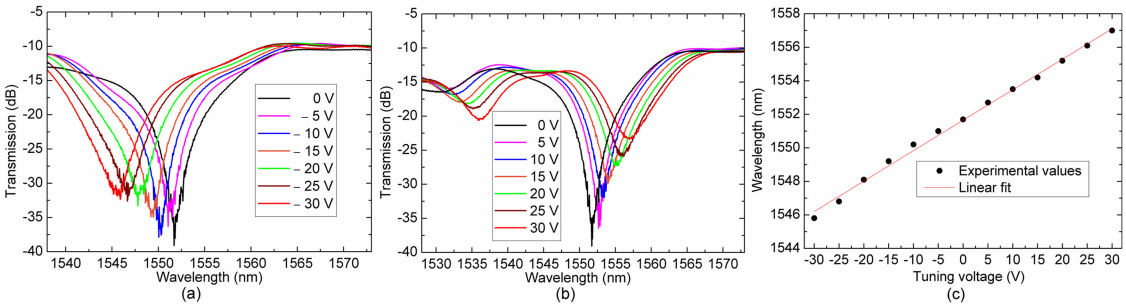

Fig. 6. Normalized transmission spectra of the TMW of the highest performance LPGADC measured at different driving voltages (a) from 0 V to –30 V, (b) from 0 V to 30 V; (c) variation of the center wavelength with the driving voltage for the rejection band.

Fig. 6(b), as the tuning voltage increases from 0 V to 30 V, the rejection band in the transmission spectrum shifts from 1551.8 nm to 1557 nm with the contrast dropping from 29 dB to 13.5 dB. The center wavelengths of the rejection band increase linearly with the increase of the tuning voltage at a rate of 0.182 nm/V, as shown in Fig. 6(c). Obviously, such a tuning functionality for the center wavelength can ease the stringent requirements in the design and fabrication of the filter. In addition, as shown in Fig. 6(a) and 6(b), the extinction ratio of the rejected band reduces with the increase of the tuning voltage, which will result in the degradation of the mode filtering performance of the device. The reduction of the extinction ratio can be attributed to the phase mismatching of the two coupled fundamental modes due to the change of the mode effective index induced by the EO tuning, which can be partly improved by improving the fabrication skill so as to reduce phase mismatching and hence achieve a larger extinction without the tuning voltage.

The propagation losses of our typical fabricated TMW with grating (i.e., the fabricated filter) were estimated by applying the cut-back method, and the results are ∼2.3 dB/cm for the LP_{01} mode in the region far from resonance wavelength and ∼2.9 dB/ cm at resonance wavelength for the LP_{11a} mode, respectively. The larger propagation loss of the fabricated filter is attributed partly to the grating as simulation result shown in Fig. 2(b) and partly to the error of the APE parameters due to imperfect fabrication process. There should be some room to reduce the loss of our device by further optimizing the design and improving the fabrication process of the device.

4. Conclusion

In summary, we have demonstrated an EO tunable LP_{01} mode filter by incorporating an LPG into an asymmetric directional coupler to compensate for the phase mismatch of the two LP_{01} modes in the SMW and TMW. Our typical fabricated device achieves a maximum mode extinction ratio of 29 dB at 1551.7 nm wavelengths, and a –20 dB bandwidth of ∼2.5 nm with an electrical wavelength tuning sensitivity of 0.182 nm/V. Our proposed mode filter offers the strength of high-speed tunable wavelength-selective mode filtering functionality, which is advantageous to ease the stringent requirements in the design and fabrication of the filter and increase the flexibility of MDM networks.

Disclosures

The authors declare no conflicts of interest.

References

[1] Q. Huang, W. Wang, W. Jin, and K. S. Chiang, “Ultra-broadband mode filter based on phase-shifted long-period grating,” *IEEE Photon. Technol. Lett.*, vol. 31, no. 13, pp. 1052–1055, Jul. 2019.
[2] Q. Huang and K. S. Chiang, “Polarization-insensitive ultra-broadband mode filter based on a 3D graphene structure buried in an optical waveguide,” *Optica*, vol. 7, no. 7, pp. 744–745, Jul. 2020.

[3] K. T. Ahmmed, H. P. Chan, and B. Li, "Broadband high-order mode pass filter based on mode conversion," *Opt. Lett.,* vol. 42, no. 18, pp. 3686–3689, Sep. 2017.
[4] C. Sun, W. Wu, Y. Yu, X. Zhang, and G. T. Reed, "Integrated tunable mode filter for a mode-division multiplexing system," *Opt. Lett.*, vol. 43, no. 15, pp. 3658–3661, Aug. 2018.
[5] M. Teng *et al.*, "Phase insensitive high order mode pass filter with low reflection for two-mode division multiplexing," in *Proc. Opt. Fiber Commun. Conf.*, 2019, Paper Th2A.5.
[6] X. Guan, Y. Ding, and L. H. Frandsen, "Ultra-compact broadband higher order-mode pass filter fabricated in a silicon waveguide for multimode photonics," *Opt. Lett.*, vol. 4, no. 16, pp. 3893–3896, Aug. 2015.
[7] Y. He, Y. Zhang, H. Wang, and Y. Su, "On-chip silicon mode blocking filter employing subwavelength-grating based contra-directional coupler," *Opt. Exp.*, vol. 26, no. 25, pp. 33005–33012, Dec. 2018.
[8] W. Shi *et al.*, "Silicon photonic grating-assisted, contra-directional couplers," *Opt. Exp.*, vol. 21, no. 3, pp. 3633–3650, Feb. 2013.
[9] H. Qiu *et al.*, "Silicon add-drop filter based on multimode grating assisted couplers," *IEEE Photon. J.*, vol. 8, no. 6, Dec. 2016, Art. no. 7805308.
[10] H. Qiu, Y. Su, P. Yu, T. Hu, J. Yang, and X. Jiang, "Compact polarization splitter based on silicon grating-assisted couplers," *Opt. Lett.*, vol. 40, no. 8, pp. 1885–1887, Apr. 2015.
[11] J. A. Davis, A. Grieco, M. C. M. M. Souza, N. C. Frateschi, and Y. Fainman, "Hybrid multimode resonators based on grating-assisted counter-directional couplers," *Opt. Exp.*, vol. 25, no. 14, pp. 16484–16490, Jul. 2017.
[12] H. Qiu *et al.*, "Silicon mode multi/demultiplexer based on multimode grating-assisted couplers," *Opt. Exp.*, vol. 21, no. 15, pp. 17904–17911, Jul. 2013.
[13] Y. Wang, K. X. Chen, L. F. Wang, and K. S. Chiang, "Sidewall-grating-assisted polymer-waveguide directional coupler for forward coupling of fundamental modes," in *Proc. Asia Commun. Photon. Conf.*, 2015, paper ASu3A.3.
[14] M. R. Zhang, W. Ai, K. X. Chen, and K. S. Chiang, "A lithium-niobate waveguide directional coupler for switchable mode multiplexing," *IEEE Photon. Technol. Lett.*, vol. 30, no. 20, pp. 1764–1767, Oct. 2018.
[15] M. R. Zhang, K. X. Chen, W. Jin, J. Y. Wu, and K. S. Chiang, "Electro-optic mode-selective switch based on cascaded three-dimensional lithium-niobate waveguide directional couplers," *Opt. Exp.*, vol. 28, no. 24, pp. 35506–35516, Nov. 2020.
[16] Q. Liu, K. S. Chiang, and V. Rastogi, "Analysis of corrugated long period gratings in slab waveguides and their polarization dependence," *J. Lightw. Technol.*, vol. 21, no. 12, pp. 3399–3405, Dec. 2003.
[17] K. S. Chiang and S. Y. Cheng, "Technique of applying the prism-coupler method for accurate measurement of the effective indices of channel waveguides," *Opt. Eng.*, vol. 47, no. 3, Mar. 2008, Art. No. 034601-4.